Clays and Clay Minerals, Vol. 34, No. 2, 136–145, 1986.

LAYER-BY-LAYER MECHANISM OF SMECTITE ILLITIZATION AND APPLICATION TO A NEW RATE LAW

CRAIG M. BETHKE AND STEPHEN P. ALTANER
Department of Geology, University of Illinois
Urbana, Illinois 61801

Abstract—A layer-by-layer mechanism explains important features of mixed-layer clay minerals formed during the illitization of smectite, including the occurrence of randomly interstratified illite/smectite, the transition to ordered interstratifications, and the development of long-range ordering. A variety of solid-state transformation mechanisms were tested with a stochastic model, which accounts for interactions among clay layers. The model produces most successful results when the reaction of smectite layers with one illite nearest neighbor is favored over smectites with no illite neighbors by a factor of about two, and over those with two illite neighbors by a factor of ten or more. Synthetic X-ray powder diffraction patterns calculated from model results compare well with those of illite/smectite minerals. These results suggest a new kinetic rate law. Solutions to this rate law for reaction within sediments undergoing burial give mineralogical profiles with depth similar to those observed in subsiding sedimentary basins.

Key Words—Illitization, Interstratification, Layer mechanism, Rate law, Smectite, Solid-state transformation.

INTRODUCTION

Many workers have observed that smectitic clay minerals tranform to illite through mixed-layer illite/smectite (I/S) intermediate products in sedimentary (Perry and Hower, 1970; Weaver and Beck, 1971; Rettke, 1976), contact metamorphic (Nadeau and Reynolds, 1981; Pytte, 1982), and hydrothermal (Steiner, 1968; McDowell and Elders, 1980; Horton, 1983; Vergo, 1984) environments. The proportion of illite to smectite layers in I/S and layer ordering progressively increase during this process, herein termed smectite illitization (Hower *et al.*, 1976; Bethke *et al.*, 1986). This reaction has been used as an indicator of thermal history (Hoffman and Hower, 1979; Nadeau and Reynolds, 1981) and may be a source of water which contributes to geopressures and petroleum migration (Powers, 1967; Burst, 1969), as well as a source of silica cement in sandstones (Towe, 1962; Boles and Franks, 1979).

Further usefulness of this transformation to understanding geological processes is limited by poor knowledge of the reaction mechanism. This paper presents a layer-by-layer mechanism of smectite illitization that explains important features of the reaction, including the occurrence of random interlayering, the transition to ordered mixed-layer minerals, and the development of long-range ordering. The results suggest a new rate law, which better describes the reaction of illitic I/S in shales than previously suggested kinetic expressions.

POSSIBLE REACTION MECHANISMS

Possible reaction mechanisms of illitization can be categorized as either solid-state or dissolution-precipitation transformations. Solid-state transformation hypotheses call on ionic substitutions of Al for Si within an intact silicate sheet, and K for exchangeable cations in the interlayer position (Towe, 1962; Weaver and Beck, 1971; Hower *et al.*, 1976). Dissolution of K-feldspar and perhaps detrital mica may supply Al and K. Pollard (1971) favored a solid-state transformation because of likely energy barriers to smectite dissolution at sub-metamorphic temperatures, and he presented a model of ionic diffusion in the interlayer region and distortion of silica tetrahedra, allowing Al substitution for Si. K/Ar dating studies that indicate that radiogenic Ar is retained within I/S minerals during illitization (Weaver and Wampler, 1970; Perry, 1974; Aronson and Hower, 1976) also support a transformation that preserves illite interlayers.

Other studies, however, support a dissolution-precipitation transformation. Boles and Franks (1979) used mineralogical data to argue that Al, instead of the silicate lattice, is conserved during illitization. This model, which requires dissolution of at least some I/S during the reaction, is supported by the data of Hower *et al.* (1976) from Gulf Coast shales, but not by Lynch and Reynolds' (1984) study of I/S in contact metamorphosed sediments. Precipitation of I/S during illitization also explains oxygen isotope equilibration of I/S with pore fluids in deeply buried samples (Eslinger and Savin, 1973; Yeh and Savin, 1977), although other explanations are possible, because oxygen isotope exchange between silicates and ground waters occurs even in coarsely crystalline minerals (Lawrence and Kastner, 1975; Taylor, 1979, pp. 248–250). Finally, based on electron micrographic study, Nadeau *et al.* (1984) suggested that I/S minerals are composed of "fundamental particles," some of which grow at the expense of others that dissolve during illitization.

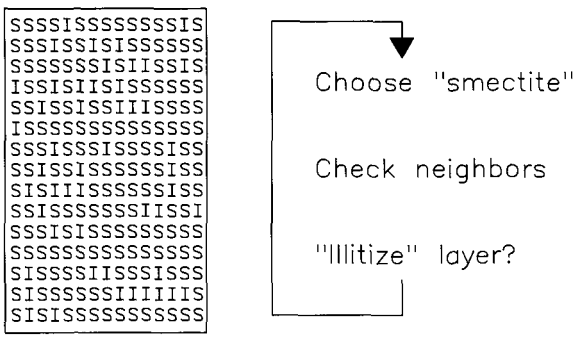

Figure 1. Monte Carlo model of smectite illitization. Model sets up hundreds of sequences of 15 smectite layers in memory of a computer, each of which represents one I/S crystallite (schematically at left). Model then randomly chooses candidate smectite layers for reaction and stochastically decides whether to transform candidates to illite, based on neighboring layers (right). Process continues until all candidates have reacted.

The present study tests layer-by-layer mechanisms of smectite illitization, assuming a solid-state transformation. The results show that a solid-state transformation mechanism can explain important features of the illitization reaction of smectite; however, they do not preclude alternate mechanisms in which dissolution and precipitation occur.

MONTE CARLO MODEL OF ILLITIZATION

Possible layer-by-layer mechanisms of smectite illitization were tested by a Monte Carlo numerical model, so-called because it employs a random number generator. Shreider (1966), Kleijnen (1974), and Yakowitz (1977) discussed stochastic techniques in detail, and Press (1968), Gilmer (1977), and Schwartz *et al.* (1983), for example, applied Monte Carlo calculations to geologic problems.

Our model (Figure 1) set up hundreds of I/S "crystallites," each of which was 15 clay (2:1) layers thick, in a computer's memory. Initially, each layer was "smectite," but in the course of the simulation, the computer randomly chose smectite layers as candidates for "illitization." The model then stochastically decided whether to illitize the candidate layer, based on the candidate's neighbors in its crystallite. The model assigned each candidate layer a probability of reacting, P, depending on its neighbors. P, which varied from zero to one, is referred to here as the layer's "reactivity." For example, smectite layers with a certain configuration of neighbors might have had a reactivity of .5. These smectites would have illitized on about half of the occasions in which they appeared as candidates. Assignment of reactivities determined the course taken by a Monte Carlo experiment.

In most of the calculations, the model assigned reactivities to candidates based on nearest-neighbor layers. Thus, candidates had either zero, one, or two illite neighbors, ignoring ends of crystallites. These are referred to as type 0, type 1, and type 2 smectites (Table 1), and reactivities for the three types are written as: $P_0/P_1/P_2$.

Table 1. Types of smectite layers based on nearest neighbors[1] and optimal reactivity values.

	Nearest neighbors	Reactivity[2]
Type 0	S$\underline{S}$S	.5
Type 1	S$\underline{S}$I & I$\underline{S}$S	1
Type 2	I$\underline{S}$I	≦.1

[1] S = smectite, I = illite.
[2] Probability.

If a candidate occurred at the end of a crystallite, the model assigned an imaginary neighbor, based on the bulk composition of the Monte Carlo clay. This procedure made results easier to present, because junction probabilities, i.e., parameters used to describe interlayering in clays (Reynolds, 1980), remained independent of position within the crystallites. Repeating successful experiments with either all illite or all smectite imaginary neighbors had little effect on model results, and end effects are probably not important to our conclusions.

Calculation results

Results of Monte Carlo experiments can be shown as pathways through junction probability diagrams, as

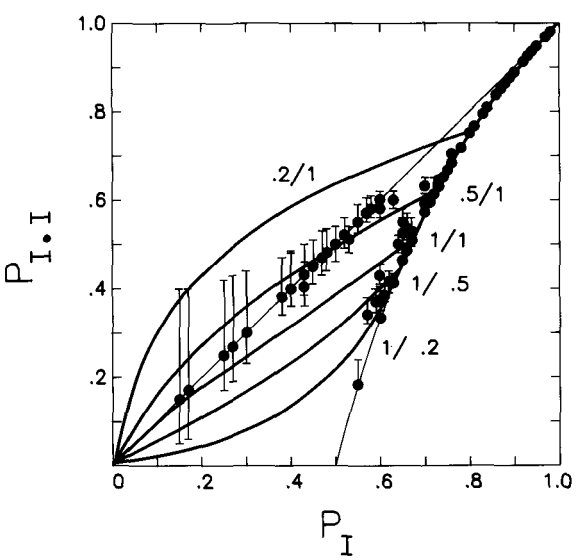

Figure 2. Pathways through a junction probability diagram taken by Monte Carlo experiments that preserve type 2 smectites until type 0 and type 1 smectites have reacted, for various ratios of P_0/P_1. Data points are mineralogical analyses of I/S from Bethke *et al.* (1986). Monte Carlo runs with reactivity ratios of about 0.5 coincide with analyses of natural samples.

https://doi.org/10.1346/CCMN.1986.0340204 Published online by Cambridge University Press

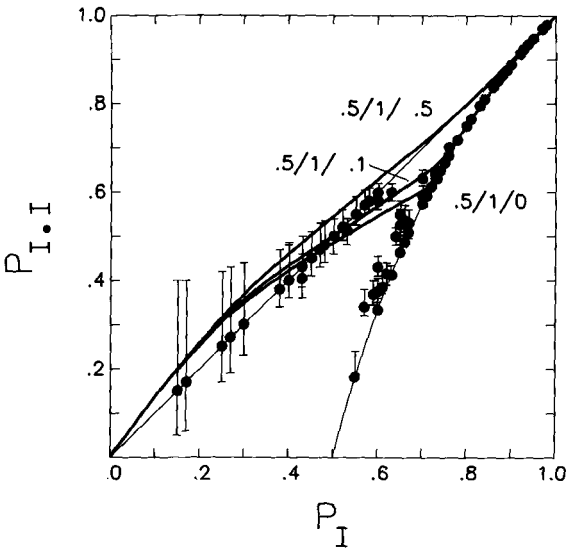

Figure 3. Pathways taken by Monte Carlo experiments with a P_0/P_1 ratio of 0.5, and varying reactivities for type 2 smectite layers. Runs with values of P_2 as great as 0.1 the value of P_1 produce good results.

described by Bethke *et al.* (1986). Figure 2 shows pathways of Monte Carlo experiments in which type 0 and type 1 smectites were illitized by varying reactivity ratios, P_0/P_1, whereas type 2 smectites were not illitized until all other smectites had reacted. Figure 2 also shows

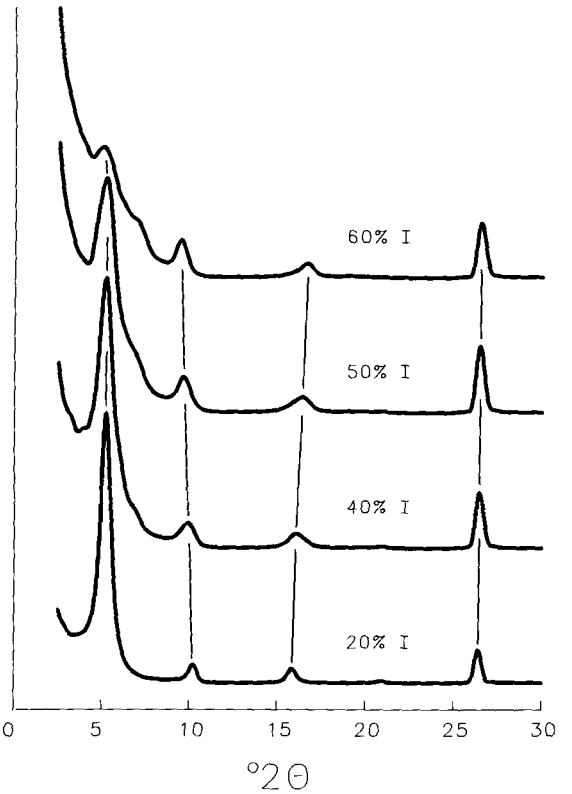

Figure 5. X-ray powder diffraction patterns calculated from Monte Carlo crystallites with 20, 40, 50, and 60% illite layers, for a run with reactivities of .5/1/.1 (CuKα radiation).

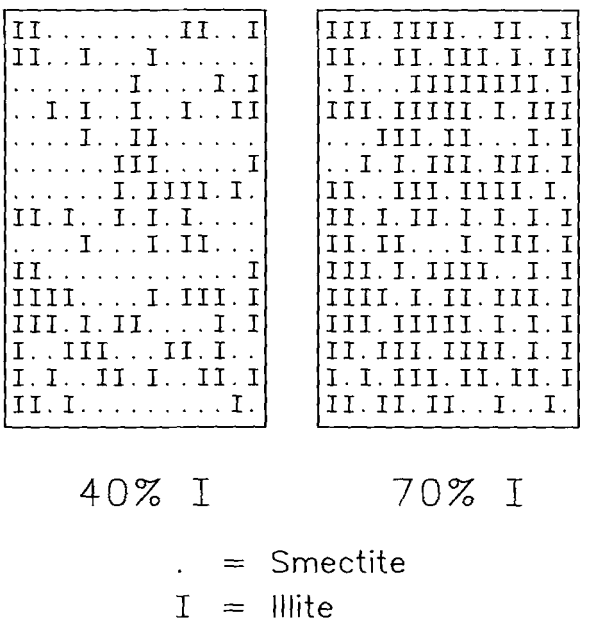

Figure 4. First 15 Monte Carlo crystallites from a run with reactivities of .5/1/.1, at 40 and 70% illite layers. Each row represents a crystallite with crystallographic c^* axis projected horizontally. Both samples show clusterings of illites and smectites; 70% sample shows little layer alternation.

mineralogical analyses of I/S from shales, bentonites, and hydrothermally altered tuffs.

Monte Carlo experiments with P_0/P_1 ratios greater than about one produced clay minerals that developed ordering at lesser illite contents than most natural I/S samples. Experiments that favored reaction of type 1 over type 0 smectites followed pathways similar to those observed in natural samples. Runs that favored type 1 smectites too greatly, however, produced segregated I/S minerals, unlike those observed in nature. The most successful Monte Carlo experiments had P_0/P_1 ratios of about 0.5.

Figure 3 shows additional Monte Carlo experiments that kept a P_0/P_1 ratio of 0.5, and relaxed the condition that type 2 smectites could not illitize until other smectites had reacted. The experiments with values of P_2 as great as one-tenth the value of P_1 followed pathways coincident with analyses of natural I/S. Larger type 2 reactivities, however, prevented the development of strong layer ordering. Table 1 shows optimal reactivity values from nearest-neighbor Monte Carlo experiments.

If smectite illitization proceeds in nature as a layer-by-layer process in which interactions among nearest neighbors predominate, smectite layers adjoining one

https://doi.org/10.1346/CCMN.1986.0340204 Published online by Cambridge University Press

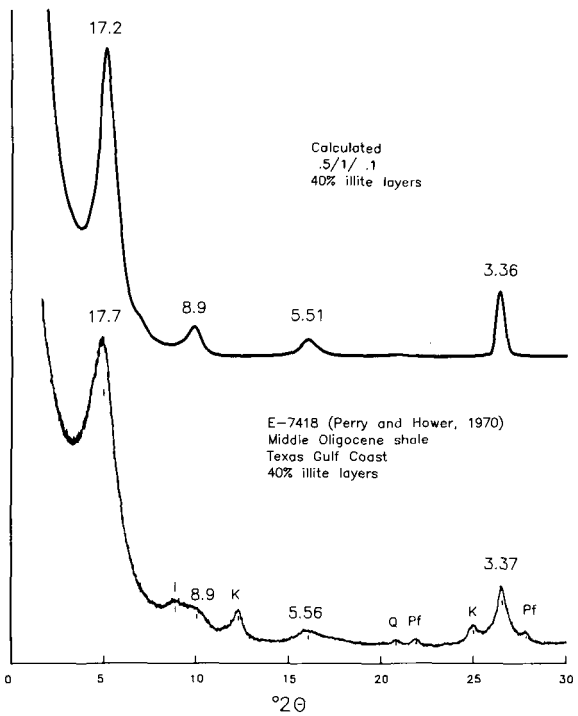

Figure 6. Comparison of calculated X-ray powder diffraction patterns of I/S with 40% illite layers (Figure 4) with pattern of randomly interlayered I/S from Gulf Coast shale cuttings. Labels show d-spacings of I/S reflections in Å, and peaks from discrete illite (I), kaolinite (K), quartz (Q), and plagioclase feldspar (Pf) (CuKα radiation).

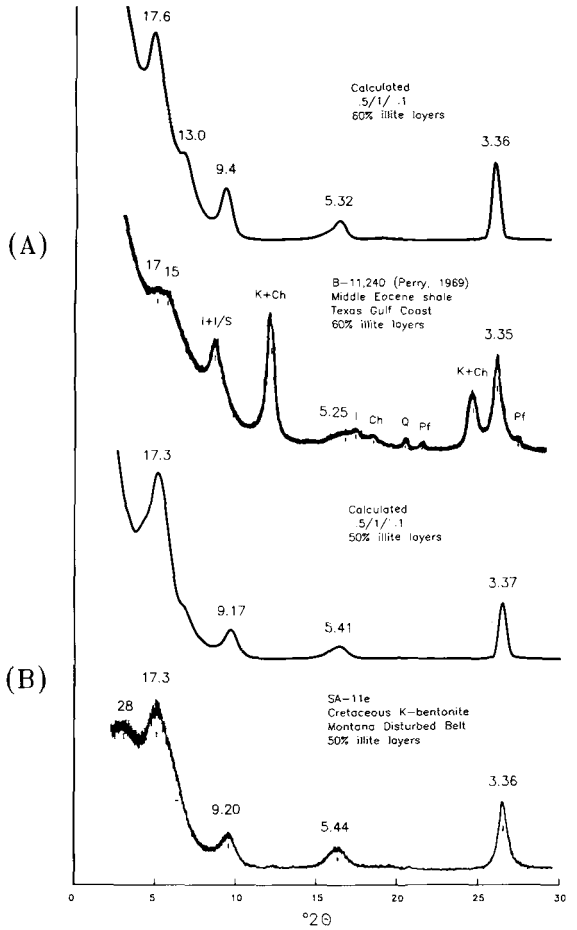

Figure 7. Calculated (Figure 4) and actual X-ray powder diffraction patterns for I/S with 50% (bottom) and 60% (top) illite layers. Ch identifies chlorite peaks. Patterns show random interstratification, with some intensity near 14 Å (CuKα radiation).

illite layer must be about twice as likely to transform to illite as those with no adjoining illites, and at least ten times as likely to react as those located between illite layers. Figure 4 shows layer arrangements produced by this reaction mechanism. Arrangements with both 40 and 70% illite show a tendency toward clustering of illite and smectite layers, and the 70% results show relatively little alternation of illite and smectite layers. Klimentidis and Mackinnon (1986) also observed common layer clustering, but uncommon layer alternation, in I/S using high-resolution transmission electron microscopy. Comparison of predicted layer distributions to HRTEM images may help further refine reaction models.

Synthetic X-ray powder diffraction patterns

To evaluate the results more carefully, XRD patterns were calculated directly from the sequences of clay layers produced by the Monte Carlo model. Calculations were made using the MOD-4 computer program (R. C. Reynolds, Dartmouth College, Hanover, New Hampshire, personal communication), modified to measure the frequency factor matrix σ directly from the Monte Carlo crystallites, instead of calculating it from junction probabilities (Bethke and Reynolds, 1986). This technique models diffraction from oriented mounts of ethylene glycol-solvated I/S in which smectite layers expand to a 16.9-Å spacing. The calculations assumed crystallite sizes of 7–13 layers. No correction was made for finite diffraction sample lengths, thus the results overestimate the diffracted intensity at low angles. All diffraction calculations assume CuKα radiation (λ = 1.5418 Å).

Figure 5 shows calculated XRD patterns of I/S with 20, 40, 50, and 60% illite layers from a Monte Carlo simulation with reactivities of .5/1/.1 (Figure 3). These patterns indicate random interstratifications of smectite and illite layers. Diffraction at 20% illite is dominated by peaks near the 001 through 005 smectite reflections. With increasing illitization, the smectite 001 reflection diminishes in intensity, the smectite 002 reflection migrates toward the position of the illite 001 reflection, and the smectite 003 reflection moves toward the illite 002 reflection.

Figures 6 and 7 show details of three of these pat-

https://doi.org/10.1346/CCMN.1986.0340204 Published online by Cambridge University Press

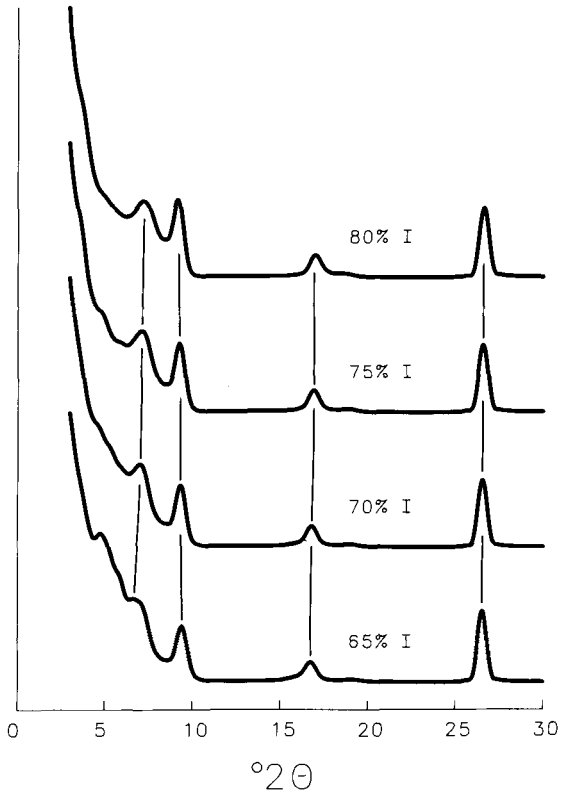

Figure 8. X-ray powder diffraction patterns calculated from Monte Carlo crystallites with 65, 70, 75, and 80% illite layers, for reactivities of .5/1/.1 (CuKα radiation).

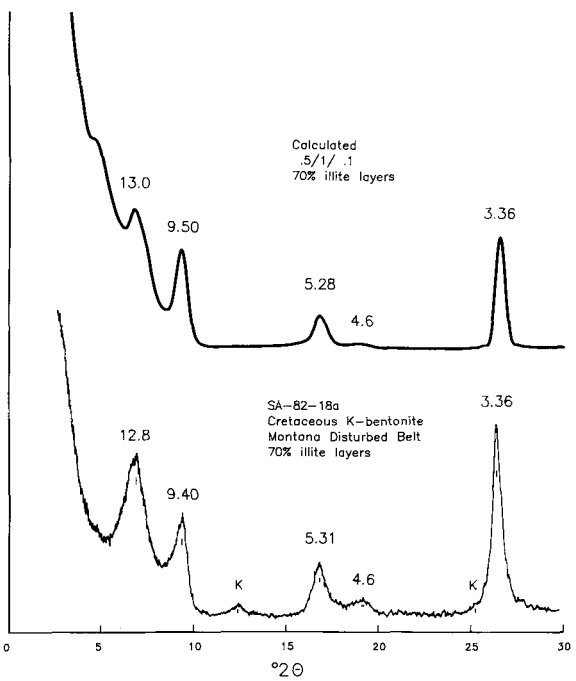

Figure 9. Calculated (Figure 8) and actual X-ray powder diffraction patterns of I/S with 70% illite layers (CuKα radiation).

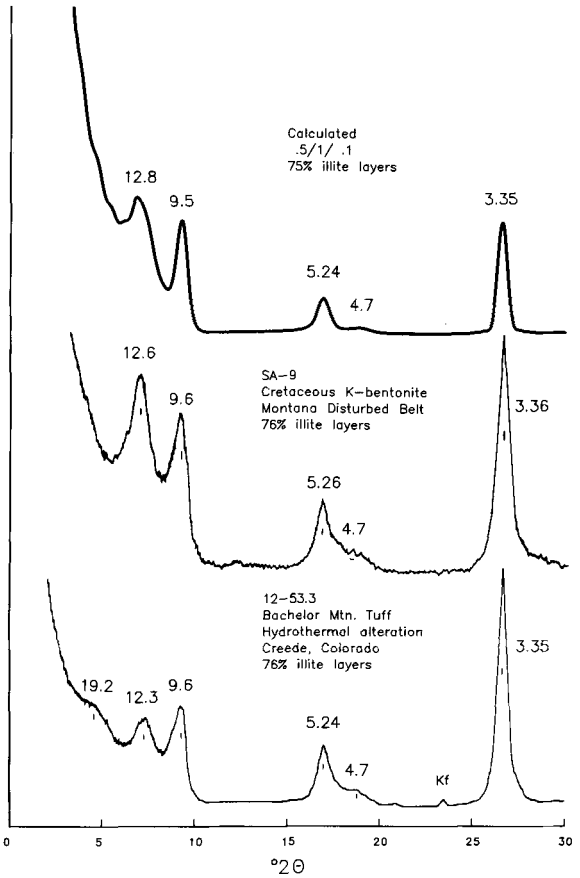

Figure 10. Calculated X-ray powder diffraction pattern for 75% illite in I/S (Figure 8), showing partial R2 ordering, and pattern of I/S from hydrothermally altered tuff, showing strong R2 ordering. Kf = potassium feldspar (CuKα radiation).

terns. An XRD pattern of a Gulf Coast shale (Perry and Hower, 1970) compares well to a calculated pattern with 40% illite layers (Figure 6). Patterns with 50 and 60% illite layers (Figure 7) show a weak reflection near 14 Å, which we interpret as the first emergence of layer ordering. XRD patterns from a Montana K-bentonite (described by Altaner, 1985) and a Gulf Coast shale (Perry, 1969) also show weak reflections near this spacing.

Calculated patterns in Figure 8 for I/S with 65, 70, 75, and 80% illite layers show development of layer ordering within the Monte Carlo crystallites. Intensity near 17 Å, evidence of random interlayering, disappears with increasing illitization, and the appearance of a low-angle peak near 13 Å indicates an emergence of layer ordering. Gradual shift of the low-angle peak toward greater 2θ signals the development of long-range ordering in the Monte Carlo clay.

The XRD pattern of Monte Carlo I/S containing 70% illite layers, plotted in Figure 9 with a Montana K-bentonite, shows a low-angle peak at 13 Å, which

https://doi.org/10.1346/CCMN.1986.0340204 Published online by Cambridge University Press

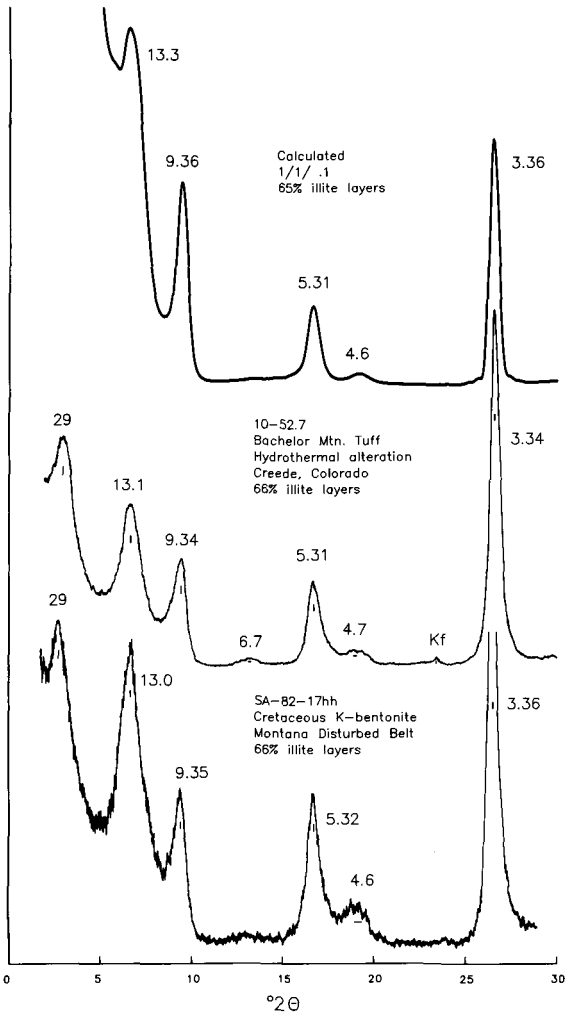

Figure 11. Calculated X-ray powder diffraction pattern of I/S with 65% illite layers from Monte Carlo run with reactivities of 1/1/.1, and of R1-ordered I/S (CuKα radiation).

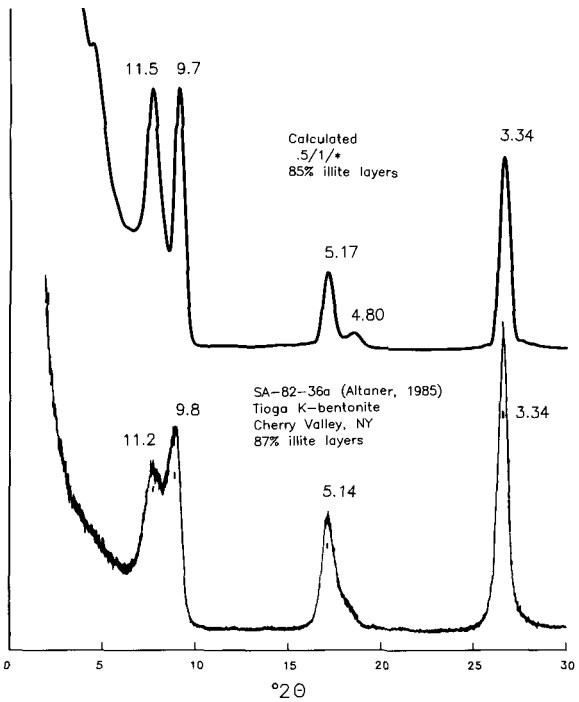

Figure 12. X-ray powder diffraction pattern resulting from removed-neighbor model of illitization, at 85% illite layers. Asterisk indicates that type 2 smectite layers were differentiated by next-nearest and thrice-removed neighbors. Calculated and actual patterns show strong R3 or Kalkberg-type order (CuKα radiation).

is interpreted as evidence of R1 or nearest-neighbor ordering. Figure 10 compares the calculated XRD pattern for I/S with 75% illite layers and the patterns of a Montana K-bentonite and a hydrothermally altered tuff (described by Vergo, 1984). The position of the superlattice peak in the calculated and K-bentonite patterns indicates R1 or R2 order, and the alteration sample shows strong R2 ordering, for comparison.

Monte Carlo runs with P_0/P_1 ratios in the range of 1 to 2, instead of 0.5, better predicted the XRD patterns of ordered I/S samples that contain $\leqq$65% illite layers. These runs gave sharper low-angle peaks, at a slightly lower angle than the .5/1/.1 pathway. Figure 11 shows a calculated pattern for I/S with 65% illite layers from the 1/1/.1 Monte Carlo experiment, plotted with R1-ordered hydrothermal alteration and K-bentonite samples.

Monte Carlo experiments which assigned reactivities based on nearest neighbors alone did not produce strong R3 ordering, such as the Kalkberg-type clays observed by Hower and Mowatt (1966) and Reynolds and Hower (1970). Calculations in which type 2 smectites were differentiated by farther removed neighbors, however, produced R3-ordered clays with very distinctive low-angle reflections. Figure 12 shows results of a removed-neighbor model in which type 0 and type 1 smectites were illitized first, using a reactivity ratio of one-half. Type 2 smectites with at least one smectite next-nearest neighbor, and later those with a thrice-removed smectite neighbor, were then allowed to react. The resulting XRD pattern of I/S with 85% illite layers is strongly R3-ordered, and compares well with Kalkberg-type I/S (Altaner, 1985).

APPLICATION TO REACTION KINETICS

Several workers have attempted to predict the extent of smectite illitization in shales as a function of time and temperature, according to a kinetic rate law. Pytte (1982) summarized arguments for considering illitization to be kinetically controlled. Whereas analogous theory seems to describe kerogen maturation (Waples, 1980), time-temperature studies of illitization do not explicitly treat effects of pore-fluid composition (Eberl

https://doi.org/10.1346/CCMN.1986.0340204 Published online by Cambridge University Press

Table 2. Differences in activation energies, $E_2 - E_1$, for reactivity ratios $P_2/P_1 \leq 0.1$.

P_2/P_1	$E_2 - E_1$ (kcal/mole)	$E_2 - E_1$ (J/mole)
1/10	1.7	7100
1/100	3.5	14,000
1/1000	5.2	21,000
1/10,000	6.9	29,000

and Hower, 1977; Eberl, 1978a, 1978b; Lahann and Roberson, 1980; Roberson and Lahann, 1981), adequacy of supply of chemical components from other minerals (Hower *et al.,* 1976; Altaner *et al.,* 1984), or the possibility of intermediate equilibrium states in the reaction (Hower *et al.,* 1976; Bruce, 1984) and should be applied with caution.

Eberl (1971) and Eberl and Hower (1976) interpreted their experimental data in terms of a pseudo-first order reaction with respect to smectite content, with an activation energy of 18–20 kcal/mole. McCubbin and Patton (1981) also fit a first-order equation to natural I/S samples with known thermal histories and found a similar activation energy. First-order laws, however, predict greater reaction rates in illitic I/S than is observed in nature. Whereas these laws suggest that illitization should proceed toward completion once moderate temperatures are attained, I/S in Gulf Coast wells actually begins to react more slowly as compositions of about 80% illite layers are reached (Perry and Hower, 1970; Hower *et al.,* 1976). This effect may be due to nature of the reaction or to the consumption of available K or Al. First-order laws also predict more complete reaction than has been observed in contact metamorphosed shales (Pytte, 1982). Pytte used rate laws of third through fifth order in smectite content and first order in K^+/Na^+ ratios set by equilibrium with sodium and potassium feldspars to show predicted reaction rates in illitic I/S. His results suggest that such laws describe I/S in contact metamorphic and diagenetic environments better than simple first-order expressions.

A first-order law which accounts for effects among neighboring layers, however, gives reasonable reaction rates, even in illitic I/S. Such an expression may be derived by writing the total rate of change in the number of smectite layers in a system as the sum of rates of change of types 0, 1, and 2 smectites

$$\frac{dN}{dt} = \frac{dN_0}{dt} + \frac{dN_1}{dt} + \frac{dN_2}{dt}. \quad (1)$$

Each type of smectite, i, is assumed to react by a first-order law

$$\frac{dN_i}{dt} = -k_i N_i, \quad (2)$$

in which the rate constant, k_i, varies with temperature according to the Arrhenius relationship

$$k_i = Ae^{-E_i/RT}. \quad (3)$$

Variables A, R, and T are the pre-exponential factor, gas constant, and absolute temperature, and E_i is the activation energy for each type of smectite layer. Combining Eqs. (1) and (2) gives the rate law

$$\frac{1}{(1 - P_I)} \frac{dP_I}{dt} = X_0k_0 + X_1k_1 + X_2k_2, \quad (4)$$

where X_i are fractions of smectite layers of each type

$$X_i = N_i/N,$$

P_I is the fraction illite layers in I/S, and the rate constants, k_i, are given by Eq. (3).

Differences among activation energies, E_i, may be estimated from results of Monte Carlo modeling. The ratio of rate constants for type 0 and type 1 smectites may be written as a quotient of Arrhenius relationships (Eq. 3), giving

$$k_0/k_1 = e^{-(E_0 - E_1)/RT}.$$

This ratio, by definition, equals the reactivity ratio, P_0/P_1, which is about 0.5 in successful models. Assuming reaction near 100°C (373 K), the difference $E_0 - E_1$, then, is about 0.5 kcal/mole (2100 J/mole). By similar argument, the activation energy difference $E_2 - E_1$ is 1.7 kcal/mole (7100 J/mole) or greater, because P_2/P_1 must be 0.1 or less. Table 2 lists activation energy differences for various values of P_2/P_1.

By setting E_1 to 18 kcal/mole, as experimentally determined for the overall reaction by Eberl (1971), the only unknown in the rate law is the pre-exponential factor. In this study, values for A of about 10^{-3}/sec gave geologically reasonable results. Due to lack of data with known thermal histories, we have not refined this value beyond the nearest order of magnitude.

Figure 13 shows solutions to the rate law (Eq. (4)) for I/S undergoing continuous burial through a geothermal gradient of 25°C/km, at various burial rates. I/S, which initially contains 10% illite layers, progressively transforms to illite during burial. Reaction rates in smectitic I/S increase with depth, due to the Arrhenius dependence of rate constants on temperature. Rates in illitic I/S, however, decrease near compositions of 75% illite layers, because of predominance of type 2 smectite layers with high activation energies. Solutions for slow burial rates predict greater degrees of illitization at shallow depths than solutions for rapid burial rates, because of longer reaction times.

Solutions to the rate law agree well with the published data of Perry and Hower (1970) and Hower *et al.* (1976). Figure 14 compares rate law solutions with data from carefully studied wells of the Texas Gulf Coast, plotted against temperature. Calculated profiles

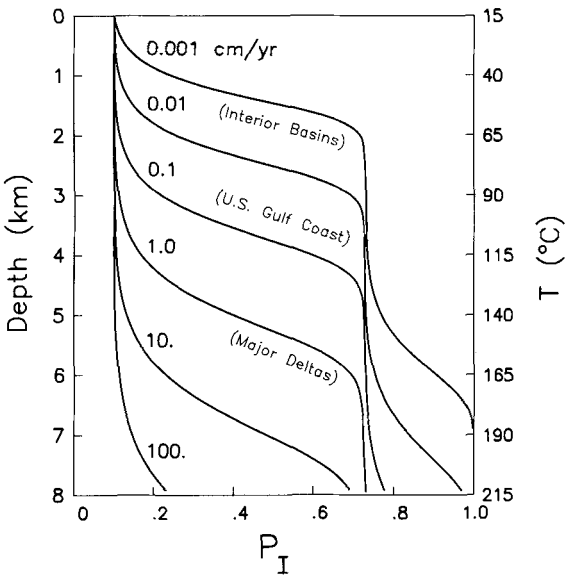

Figure 13. Solutions to rate law (Eq. (4)) for sediments undergoing burial through 25°C/km geothermal gradient, at various burial rates. Plots show fraction illite layers in I/S vs. depth and temperature. Calculations use activation energies of 18.5, 18, and 24 kcal/mole for types 0, 1, and 2 smectite layers, and a pre-exponential factor of 10^{-3}/sec.

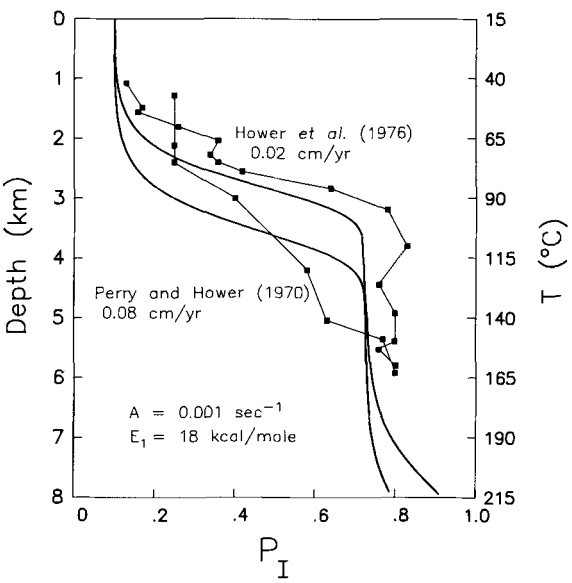

Figure 14. Comparison of rate law solutions to observed illite content of I/S, from Gulf Coast wells (Perry and Hower, 1970; Hower *et al.*, 1976). Fraction illite layers in I/S is plotted vs. depth and temperature.

assume a geothermal gradient of 25°C/km and burial rates of 0.08 and 0.02 cm/yr, as estimated from well depths and formation ages.

DISCUSSION

Results of Monte Carlo modeling demonstrate that important features of the illitization reaction of smectite can be explained by a layer-by-layer model of a solid-state transformation. Calculations which account for interaction among neighboring layers in I/S crystallites show development of random interlayering and transition to short-range (and then long-range) ordered interstratifications.

In successful Monte Carlo runs, an illite neighbor acts to increase reactivity of a smectite layer, whereas two illite neighbors sharply decrease smectite reactivity, thereby suggesting that two or more interactions among layers compete during illitization. For example, illite neighbors may act as "templates" that lower energy barriers to reaction of a smectite layer. Two illite neighbors, however, may polarize charge density in silicate sheets on both sides of smectite interlayers (Sawhney, 1969), causing resistance to potassium fixation.

Calculations that account for effects of removed neighbors on smectite layer reactivity better explain development of long-range ordering in I/S. A comprehensive model of smectite illitization might include all possible interactions among removed neighbors, but, due to the number of variables involved, these calculations are beyond the scope of this paper. In addition, smectite reactivities are unlikely to remain constant during illitization, because reaction commonly occurs over a range of temperatures and chemical environments. Non-linear reaction models are difficult to test, however, because functional forms of reactivities are unknown.

Synthetic XRD patterns from results of Monte Carlo modeling compare well with XRD patterns from natural I/S. Our calculations have the advantage of predicting patterns from suites of I/S minerals of varying composition and layer ordering, but techniques of Reynolds and Hower (1970) and Reynolds (1980) can model diffraction from a specific mineral as well, or more accurately.

Finally, solutions to a rate law suggested by the Monte Carlo modeling (Figure 13) show moderate dependence of illitization profiles in subsiding basins on burial rate. The rate law predicts illitization occurring at shallower depths and over smaller depth intervals in slowly subsiding than in rapidly subsiding basins. This result may explain why Huff and Türkmenöglü (1981) observed highly illitized I/S in Ordovician sediments of the Cincinnati arch, which have never been heated to temperatures associated with illitization in the Gulf Coast, while Ramseyer (1984) described I/S with 80% smectite layers in Miocene sediments buried to more than 4 km in the San Joaquin Valley. These examples, however, are nearly geologic extremes of the thermal histories which a sediment could follow, and less dramatic variation in sedimentation rate leads to only slightly different predicted profiles.

ACKNOWLEDGMENTS

This study arose from many discussions with G. W. Brindley. We appreciate assistance from N. Vergo, R. C. Reynolds, J. Hower, and R. J. Kirkpatrick. N. Vergo provided unpublished powder XRD patterns of I/S from hydrothermally altered tuffs. ARCO Oil and Gas Company, Exxon Production Research Company, and the University of Illinois Research Board sponsored this research. Terri Monnett typed the manuscript. We thank D. D. Eberl, R. C. Reynolds, J. Środoń, and R. K. Stoessell for thoughtful reviews of the manuscript.

REFERENCES

Altaner, S. P. (1985) Potassium metasomatism and diffusion in Cretaceous K-bentonites from the disturbed belt, northwestern Montana and in the Middle Devonian Tioga K-bentonite, eastern U.S.A.: Ph.D. dissertation, Univ. of Illinois, Urbana, Illinois, 193 pp.

Altaner, S. P., Whitney, G., Aronson, J. L., and Hower, J. (1984) A model for K-bentonite formation, evidence from zoned K-bentonites in the disturbed belt, Montana: *Geology* **12,** 412–415.

Aronson, J. L. and Hower, J. (1976) Mechanism of burial metamorphism of argillaceous sediments, 2. Radiogenic argon evidence: *Geol. Soc. Amer. Bull.* **87,** 738–744.

Bethke, C. M. and Reynolds, R. C. (1986) Recursive method for determining frequency factors in interstratified clay diffraction calculations: *Clays & Clay Minerals* **34,** 224–226.

Bethke, C. M., Vergo, N., and Altaner, S. P. (1986) Pathways of smectite illitization: *Clays & Clay Minerals* **34,** 125–135.

Boles, J. R. and Franks, S. G. (1979) Clay diagenesis in Wilcox sandstones of southwest Texas, implications of smectite diagenesis on sandstone cementation: *J. Sed. Petrol.* **49,** 55–70.

Bruce, C. H. (1984) Smectite dehydration, its relation to structural development and hydrocarbon accumulation in northern Gulf of Mexico Basin: *Amer. Assoc. Petrol. Geol. Bull.* **68,** 673–683.

Burst, J. F. (1969) Diagenesis of Gulf Coast clayey sediments and its possible relation to petroleum migration: *Amer. Assoc. Petrol. Geol. Bull.* **53,** 73–93.

Eberl, D. D. (1971) Experimental diagenetic reactions involving clay minerals: Ph.D. dissertation, Case Western Reserve Univ., Cleveland, Ohio, 145 pp.

Eberl, D. (1978a) The reaction of montmorillonite to mixed-layer clay, the effect of interlayer alkali and alkaline earth cations: *Geochim. Cosmochim. Acta* **42,** 1–7.

Eberl, D. (1978b) Reaction series for dioctahedral smectites: *Clays & Clay Minerals* **26,** 327–340.

Eberl, D. and Hower, J. (1976) Kinetics of illite formation: *Geol. Soc. Amer. Bull.* **87,** 1326–1330.

Eberl, D. and Hower, J. (1977) The hydrothermal transformation of sodium and potassium smectite into mixed-layer clay: *Clays & Clay Minerals* **25,** 215–227.

Eslinger, E. V. and Savin, S. M. (1973) Mineralogy and oxygen isotope geochemistry of the hydrothermally altered rocks of the Ohaki-Broadlands, New Zealand geothermal area: *Amer. J. Sci.* **273,** 207–239.

Gilmer, G. H. (1977) Computer simulation of crystal growth: *J. Crystal Growth* **42,** 3–10.

Hoffman, J. and Hower, J. (1979) Clay mineral assemblages as low-grade metamorphic geothermometers, application to the thrust faulted disturbed belt of Montana, U.S.A.: *Soc. Econ. Paleont. Mineral. Special Paper* **26,** 55–79.

Horton, D. G. (1983) Argillic alteration associated with the Amethyst vein system, Creede Mining District: Ph.D. dissertation, Univ. of Illinois, Urbana, Illinois, 337 pp.

Hower, J., Eslinger, E. V., Hower, M., and Perry, E. A. (1976) Mechanism of burial metamorphism of argillaceous sediments, 1. Mineralogical and chemical evidence: *Geol. Soc. Amer. Bull.* **87,** 725–737.

Hower, J. and Mowatt, T. C. (1966) The mineralogy of illites and mixed-layer illite/montmorillonites: *Amer. Mineral.* **51,** 825–854.

Huff, W. D. and Türkmenöglü, A. G. (1981) Chemical characteristics and origin of Ordovician K-bentonites along the Cincinnati arch: *Clays & Clay Minerals* **29,** 113–123.

Kleijnen, J. P. C. (1974) *Statistical Techniques in Simulation:* Dekker, New York, 775 pp.

Klimentidis, R. E. and Mackinnon, I. D. R. (1986) High-resolution imaging of ordered mixed-layer clays: *Clays & Clay Minerals* **34,** 155–164.

Lahann, R. W. and Roberson, H. E. (1980) Dissolution of silica from montmorillonite, effect of solution chemistry: *Geochim. Cosmochim. Acta* **44,** 1937–1943.

Lawrence, J. R. and Kastner, M. (1975) O^{18}/O^{16} of feldspars in carbonate rocks: *Geochim. Cosmochim. Acta* **39,** 97–102.

Lynch, L. and Reynolds, R. C. (1984) The stoichiometry of the smectite-illite reaction: *Program and Abstracts, Clay Minerals Society 21st Ann. Meeting, Baton Rouge, Louisiana, 1984,* p. 84.

McCubbin, D. G. and Patton, J. W. (1981) Burial diagenesis of illite/smectite, a kinetic model: *Bull. Amer. Assoc. Petrol. Geol.* **65,** p. 956 (abstract).

McDowell, S. D. and Elders, W. A. (1980) Authigenic layer silicate minerals in borehole Elmore 1, Salton Sea geothermal field, California, USA: *Contributions Mineral. Petrol.* **74,** 293–310.

Nadeau, P. H. and Reynolds, R. C. (1981) Burial and contact metamorphism in the Mancos shale: *Clays & Clay Minerals* **29,** 249–259.

Nadeau, P. H., Wilson, M. J., McHardy, W. J., and Tait, J. M. (1984) Interstratified clays as fundamental particles: *Science* **225,** 923–925.

Perry, E. A. (1969) Burial diagenesis in Gulf Coast pelitic sediments: Ph.D. dissertation, Case Western Reserve Univ., Cleveland, Ohio, 121 pp.

Perry, E. A. (1974) Diagenesis and K/Ar dating of shales and clay minerals: *Geol. Soc. Amer. Bull.* **85,** 827–830.

Perry, E. and Hower, J. (1970) Burial diagenesis in Gulf Coast pelitic sediments: *Clays & Clay Minerals* **18,** 165–177.

Pollard, C. O. (1971) Semidisplacive mechanism for diagenetic alteration of montmorillonite layers to illite layers: appendix to Weaver, C. E. and Beck, K. C., Clay water diagenesis during burial, how mud becomes gneiss: *Geol. Soc. Amer. Special Paper* **134,** 79–93.

Powers, M. C. (1967) Fluid release mechanisms in compacting marine mudrocks and their importance in oil exploration: *Amer. Assoc. Petrol. Geol. Bull.* **51,** 1240–1254.

Press, F. (1968) Earth models obtained by Monte Carlo inversion: *J. Geophys. Res.* **73,** 5223–5234.

Pytte, A. M. (1982) The kinetics of the smectite to illite reaction in contact metamorphic shales: M.A. thesis, Dartmouth College, Hanover, New Hampshire, 78 pp.

Ramseyer, K. U. (1984) The occurrence of highly expanded mixed-layer I/S-clays in deep Tertiary cores, San Joaquin Valley, California: *Program and Abstracts, Clay Minerals Society, 21st Ann. Meeting, Baton Rouge, Louisiana, 1984,* p. 96.

Rettke, R. C. (1976) Clay mineralogy and clay mineral distribution patterns in Dakota Group sediments, northern Denver Basin, eastern Colorado and western Nebraska:

Ph.D. dissertation, Case Western Reserve Univ., Cleveland, Ohio, 135 pp.

Reynolds, R. C. (1980) Interstratified clay minerals: in *Crystal Structures of Clay Minerals and their X-ray Identification,* G. W. Brindley and G. Brown, eds., Mineralogical Society, London, 249–303.

Reynolds, R. C. and Hower, J. (1970) The nature of interlayering in mixed-layer illite-montmorillonites: *Clays & Clay Minerals* **18,** 25–36.

Roberson, H. E. and Lahann, R. W. (1981) Smectite to illite conversion rates, effect of solution chemistry: *Clays & Clay Minerals* **29,** 129–135.

Sawhney, B. L. (1969) Regularity of interstratification as affected by charge density in layer silicates: *Soil Sci. Soc. Amer. Proc.* **33,** 42–46.

Schwartz, F. W., Smith, L., and Crowe, A. S. (1983) A stochastic analysis of macroscopic dispersion in fractured media: *Water Resources Res.* **19,** 1253–1265.

Shreider, Y. A. (1966) *The Monte Carlo Method:* Pergamon Press, New York, 381 pp.

Steiner, A. (1968) Clay minerals in hydrothermally altered rocks at Wairakei, New Zealand: *Clays & Clay Minerals* **16,** 193–213.

Taylor, H. P. (1979) Oxygen and hydrogen isotope relationships in hydrothermal mineral deposits: in *Geochemistry of Hydrothermal Ore Deposits,* 2nd ed., H. L. Barnes, ed., Wiley, New York, 236–277.

Towe, K. M. (1962) Clay mineral diagenesis as a possible source of silica cement in sedimentary rocks: *J. Sed. Petrol.* **32,** 26–28.

Vergo, N. (1984) Wallrock alteration at the Bulldog Mountain mine, Creede mining district, Colorado: M.S. thesis, Univ. of Illinois, Urbana, Illinois, 88 pp.

Waples, D. W. (1980) Time and temperature in petroleum formation, application of Lopatin's method to petroleum exploration: *Amer. Assoc. Petrol. Geol. Bull.* **64,** 916–926.

Weaver, C. E. and Beck, K. C. (1971) Clay water diagenesis during burial, how mud becomes gneiss: *Geol. Soc. Amer. Special Paper* **134,** 96 pp.

Weaver, C. E. and Wampler, J. M. (1970) K, Ar, illite burial: *Geol. Soc. Amer. Bull.* **81,** 3423–3430.

Yakowitz, S. J. (1977) *Computational Probability and Simulation:* Addison-Wesley, Reading, Massachusetts, 240 pp.

Yeh, H.-W. and Savin, S. M. (1977) Mechanism of burial metamorphism of argillaceous sediment, 3. Oxygen isotope evidence: *Geol. Soc. Amer. Bull.* **88,** 1321–1330.

(Received 12 February 1985; accepted 3 July 1985; Ms. 1462)